

Proximity hybridization induced molecular machine for signal-on electrochemical detection of α -synuclein oligomers

Qisheng Luo^a, Zhili Qiu^b, Hongqu Liang^a, Fa Huang^a, Chen Wei^a, Jiuying Cui^c, Zichun Song^c, Qianli Tang^a, Xianjiu Liao^{c,*}, Zhao Liu^{d,***}, Jiangbo Wang^{e,f,****}, Fenglei Gao^{b,*}

^a The Affiliated Hospital of Youjiang Medical University for Nationalities, Baise, Guangxi, 533000, China

^b School of Pharmacy, Xuzhou Medical University, 221004, Xuzhou, China

^c West Guangxi Key Laboratory for Prevention and Treatment of High-incidence Diseases, Youjiang Medical University for Nationalities, Baise, Guangxi, 533000, China

^d Department of Thyroid and Breast Surgery, Affiliated Hospital of Xuzhou Medical University, 221004, Xuzhou, China

^e Department of Neurology, Xuzhou Central Hospital, 221004, Xuzhou, China

^f Xuzhou Institute of Cardiovascular Disease, 221004, Xuzhou, China

ARTICLE INFO

Handling editor: J.-M. Kauffmann

Keywords:

Proximity hybridization

DNA walker

Signal-on

ABSTRACT

α -synuclein oligomer is a marker of Parkinson's disease. The traditional enzyme-linked immunosorbent assay for α -synuclein oligomer detection is not conducive to large-scale application due to its time-consuming, high cost and poor stability. Recently, DNA-based biosensors have been increasingly used in the detection of disease markers due to their high sensitivity, simplicity and low cost. In this study, based on the DNAzyme-driven DNA bipedal walking method, we developed a signal-on electrochemical sensor for the detection of α -syn oligomers. Bipedal DNA walkers have a larger walking area and faster walking kinetics, providing higher amplification efficiency compared to conventional DNA walkers. The DNA walker is driven via an Mg^{2+} -dependent DNAzyme, and the binding-induced DNA walker will continuously clamp the MB, resulting in the proliferation of Fc confined near the GE surface. The linear range and limit of detection were 1 fg/mL to 10 pg/mL and 0.57 fg/mL, respectively. The proposed signal-on electrochemical sensing strategy is more selective. It will play a significant role in the sensitive and precise electrochemical analysis of other proteins.

1. Introduction

Parkinson's disease and Alzheimer's disease are prevalent neurodegenerative disorders in the elderly, characterized by abnormalities in α -synuclein oligomers that can be detected in the cerebrospinal fluid of patients and plasma [1,2,3]. The detection of α -syn oligomer has the potential to aid in the early detection of various neurodegenerative disorders [4,5]. Currently, instrumental detection has been employed to determine the α -syn oligomer, such as capillary electrophoresis, mass spectrum, enzyme-linked immunosorbent assay and atomic force microscopy [6–8]. However, these methods are often costly, time-consuming due to complex sample pretreatment requirements, and require skilled operators [9,10]. Therefore, it is crucial to develop cost-effective and user-friendly detection methods for early diagnosis of

these diseases.

The electrochemical approach, one of many available methods for the detection of α -syn oligomers, has the advantages of simplicity and speed as well as being a more affordable alternative method for instrumental analysis. It is especially appropriate for the detection requirements of large sample series. Traditional electrochemical biosensors use target proteins to induce changes in the electrochemical signal to "turn the signal on or off" on the electrode surface [11–15]. In recent years, the development of electrochemical DNA sensors has attracted much attention. These sensors enable signal switching on and off by detecting hybridization-induced conformational changes by binding probe DNA on redox-labeled modified electrodes [16–20]. In contrast, "signal on" sensors can achieve better signal performance because the background current is reduced in the absence of the target.

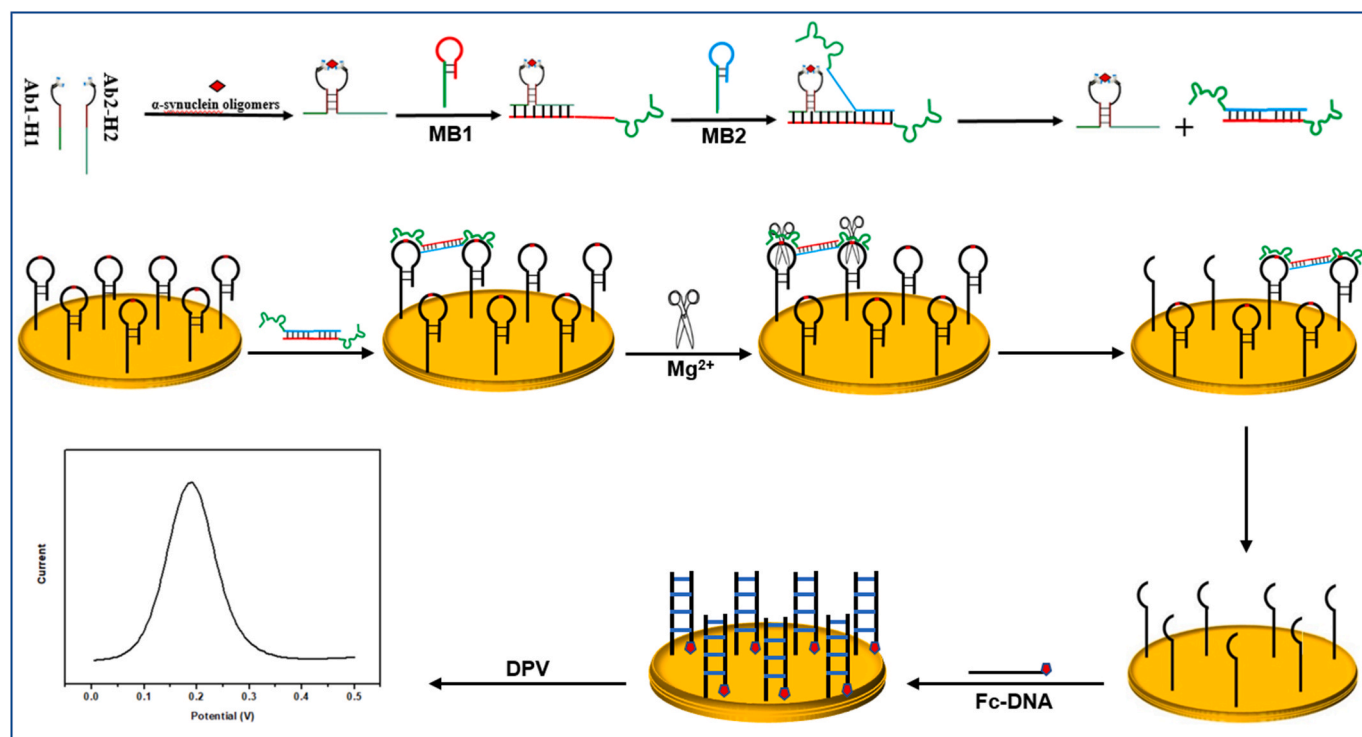
* Corresponding author.

** Corresponding author.

*** Corresponding author.

**** Corresponding author.

E-mail addresses: lxj2006910@163.com (X. Liao), xylzhao9999@163.com (Z. Liu), wangjiangbo2011@126.com (J. Wang), jsxzgf@sina.com (F. Gao).



Scheme 1. Principle of the electrochemical sensor based on the DNAzyme-driven bipedal DNA walker strategy for α -syn oligomer detection.

There is no theoretical limit to the gain of this type of sensor; therefore, many studies based on "signal-on" E-DNA architectures have been carried out [21–25]. In addition, existing "signal on" sensors are less sensitive to the target because each target DNA molecule reacts with only one signal probe, which limits the overall signal gain. Our prior work has proved the high performance of sensing platforms based on signal-on detection technology. Moreover, the high accuracy of combining signal on detection with DNA walker-based sensing has not been reported because the concentrations of disease-related biomarkers are often found in lower concentrations [26–29].

As a molecular machine, DNA walkers can operate particular DNA (walking strands) to automatically move following the programmed oligonucleotide tracks [30–33]. Usually, DNA walkers are driven by strand displacement, protein enzymes and DNAzymes [34,35]. The walker's movements have the potential to destroy the tracks and produce single-stranded products for signal amplification that can be employed as transducers in analytical and diagnostic applications [36]. Currently, most DNA walkers have only one walking strand, or single-legged DNA walkers, which causes poor reaction kinetics and restricted walking area [37]. The same matrix multipedal DNA walkers were developed by linking many walking strands together to obtain high processing speed and fast response [38]. The growing number of "legs" has greatly increased the pace or distance of walking [39]. Based on the above analysis, we developed a new style of electrochemical signal-on immunosensor based on proximity hybridization induced bipedal DNA walker driven by DNAzyme.

In contrast to affinity ligands that rely on simultaneous recognition of target proteins by two DNA-bound affinity ligands or antibody-based proximity detection [40–47], bipedal DNA walkers are a method that utilizes toehold exchange reaction drive to move across functional electrodes of orbital chains. This procedure does not require the involvement of enzymes, is simple to operate, and the reaction is not readily influenced by the surrounding environment. The combination of DNAzyme signal amplification and bipedal DNA walker boosts detection sensitivity, fits the clinical detection needs, and has high application potential. This integrated approach provides new ideas for the design of

analytical methods for electrochemical sensors.

2. Materials and methods

2.1. Materials

N-succinimidyl 4-(maleimidomethyl)cyclo-hexanecarboxylate (SMCC), sulfuric acid (H_2SO_4), hydrogen peroxide (H_2O_2), 2-Mercaptoethanol (MCH), high-density lipoprotein (HDL), potassium ferricyanide ($\text{K}_3\text{Fe}(\text{CN})_6$), glucose (Glu), and magnesium chloride (MgCl_2) were purchased from Shanghai Aladdin Biochemical Technology Co., Ltd. amyloid- β fibers ($\text{A}\beta\text{F}$), amyloid- β monomer ($\text{A}\beta\text{M}$), immunoglobulin G (IgG) and L-cysteine were obtained from Sigma-Aldrich (St. Louis, MO, U.S.A.). Synuclein Oligomer were purchased from Wuhan Huamei Biological Co. The oligonucleotides were synthesized and purified by Shanghai Sangon Biotech Co., LTD. The supporting data contained information about the DNA oligonucleotides utilized in this work.

2.2. Probes of Ab-H2 and Ab-H1

Prior investigations were carried out in order to synthesize the probe: DNA-labeled antibodies (Ab-H1 or Ab-H2). First, anti- α -syn oligomer antibody (3 mg mL^{-1}) was initially treated for 1.5 h at ambient temperature within PBS containing a 15-fold molar excess of N-succinimidyl 4-(maleimidomethyl)cyclo-hexanecarboxylate (SMCC). Simultaneous activation of the mercapto-group at the end of H1 was performed by incubating $4 \mu\text{L}$ (150 mM) dithiothreitol (DTT) with 3 mL (150 mM) H1 in PBS about 1.5 h at 37°C . An ultrafiltration process was performed on both products utilizing a Millipore membrane with a $10,000 \text{ MW}$ cutoff. After that these products were mixed well in PBS and incubated at 4°C about 24 h, then the excess DNA was filtered out by ultrafiltration to obtain Ab-H1.

2.3. Fabrication of sensors

The polished bare gold electrode (GE) were cleaned with deionized

water, ethanol, then deionized water in that order. Nitrogen gas was then used to dry them. Following that, the chips were submerged for 30 s in a moderate piranha solution ($\text{H}_2\text{SO}_4/30\% \text{H}_2\text{O}_2 = 3:1$) to eliminate contaminants in order to prepare it for modification. Then the polished GE was cleaned ultrasonically in distilled water. Following that, we dropped 10 μL MB3 (1 μM) to GE in the dark for 3 h. The unreacted MB3 was filtered out by distilled water.

2.4. Fabrication procedure of the bipedal DNA walker

To make bipedal DNA walkers, 10 μL of varying quantities of target α -syn oligomers were combined with 5 μL Ab-H1/Ab-H2, 5 μL MB1, and 5 μL MB2 for about 50 min to self-assemble the bipedal DNA walker. Subsequently, 5 μL of the mixture was added to the pre-treated GE, and to ensure that the reaction proceeded, we added tris buffer containing Mg^{2+} (2.5 mM). Under these reaction conditions, we performed a 2-h incubation. Then the Fc-DNA (7 μL , 1 μM) probe was applied to the basal surface and let stand for 30 min in 37 $^\circ\text{C}$. The substrate was then rinsed with buffer and stored at 4 $^\circ\text{C}$ in the dark for later use. Then, Fc-DNA (7 μL , 1 μM) were placed to the surface of the substrate and incubated for 30 min at 37 $^\circ\text{C}$. After that, the substrate should be rinsed with buffer and stored in the dark at 4 $^\circ\text{C}$ for future usage.

2.5. Measurement procedure

In the potential range -560 to -60 mV vs. Ag/AgCl, we recorded the differential pulse voltammetry (DPV) measurements of the electrode (pulse width and amplitude of 200 ms and 50 mV, respectively). 0.1 M KCl and 1.0 mM $\text{K}_3[\text{Fe}(\text{CN})_6]/\text{K}_4[\text{Fe}(\text{CN})_6]$ (1:1) solution were prepared as the supporting electrolyte solution. Electrochemical Impedance Spectroscopy (EIS) measurements were made at alternating current voltage frequencies ranging from 100 kHz to 100 mHz, with an amplitude of 5 mV. The voltage used in this experiment was 172 mV vs. Ag/AgCl.

3. Results and discussion

3.1. Process and mechanism of the analysis

The analytic process of α -syn oligomer took were demonstrated in Scheme 1. The proximity α -syn oligomer-DNA complex was created as a result of α -syn oligomer's partial hybridization with Ab-H1 and Ab-H2, which led to the unraveling of MB1's hairpin structure and the exposure of its initially concealed toehold region. Due to the enthalpy-driven catalytic hairpin assembly (CHA), the exposed toehold region of MB1 results in the opening of MB2 and the shedding of the " α -syn oligomer-DNA" complex from MB1 as the strand shift reaction proceeds. The detached complex is released for the succeeding cycle of reactions in order to maintain a consistent and spontaneous cyclical process. The bare toehold sequence of MB2 is hybridized with MB1 and yields the bipedal DNA walker (MB1-MB2). The bipedal DNA walker was then hybridized on the substrate with the stationary MB3, which led to the formation of the Mg^{2+} -dependent DNAzyme. The walker then hybridizes with MB3 to produce an Mg^{2+} -dependent DNAzyme. In the presence of magnesium ions, MB3 will be cleaved into two segments and the free end of the bipedal DNA walker is released. Following that, the bipedal DNA walker cleaves the spatially neighboring other MB3 and proceeds to hybridize with more MB3, forming a greater number of MB3 splinters. MB3 fragment structures assembles with the ferrocene (Fc)-labeled DNA. The large amount of Fc on the electrode surface results in a substantial electron transfer, forming a detectable redox current. The signal on electrochemical method provided precise and sensitive measurement.

3.2. Characterization of the modified GE

The assembly and operation of the sensor were measured and

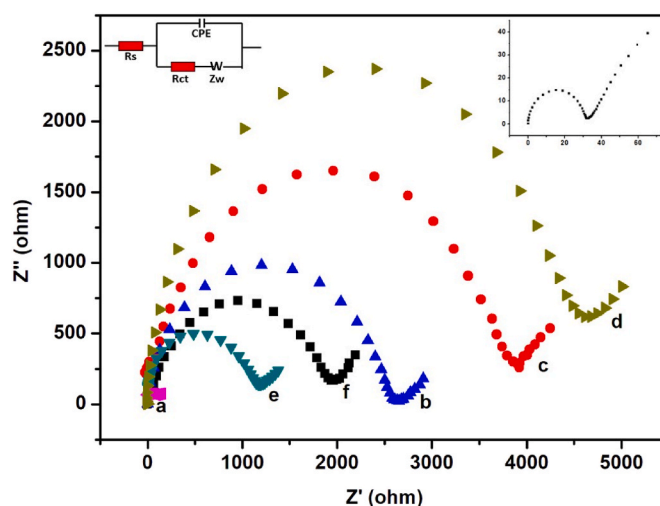


Fig. 1. (A) EIS characterization for the preparation of the electrochemical sensor at various phases: (a) Bare GE; (b) MB3/GE; (c) MCH/MB3/GE; (d) bipedal DNA walker/MCH/MB3/GE; (e) Mg^{2+} /bipedal DNA walker/MCH/MB3/GE; (f) Fc-DNA/ Mg^{2+} /bipedal DNA walker/MCH/MB3/GE; Inset: the magnification of curve a and standard Randles circuit.

characterized by EIS. Fig. 1 depicts the impedance spectra of the altered substrate at various timeframes. On the initial GE, we found a very small semicircle domain (curve a), which indicates that GE is very clean after treated with piranha solution and the charged ions generated by $[\text{Fe}(\text{CN})_6]^{3-/4-}$ can be rapidly conducted to the GE surface. The Ret value spiked after MB3 was placed onto the substrate surface (curve b). This is because the electrostatic repulsion between the negatively charged $[\text{Fe}(\text{CN})_6]^{3-/4-}$ redox probe and GE interface prevents the interfacial charge transfer. It is noteworthy that the Ret value increases more with the addition of non-conductive MCH (curve c). Interfacial electron transfer of redox probes is gradually hindered due to the buildup of negatively charged phosphate skeletons on GE. After the bipedal DNA walker was added and bond together with MB3, the Ret value increased significantly (curve d). Regardless, when numerous MB3 split in the presence of Mg^{2+} , the Ret value reduced (curve e). After Fc-DNA reporters were modified on the GE, the resistance increased (curve f), which is ascribed to the fact that Fc-DNA could greatly restrict the effective surface area of the electrode which allows the electron transfer. The above-mentioned test impedance data indicates that the sensor was effectively constructed and can operate in an orderly manner as designed.

3.3. Verification of the manufacturing process of the sensor

The effectiveness of our method for detecting human α -syn oligomers was shown by detecting the electrochemical response of the sensor device. When exposed to human α -syn oligomer, the sensor's electrochemical intensity reactions are shown in Fig. 2A. Through a number of experiments including controls, the reaction was found. Indicating the development of bipedal DNA walkers, the electrochemical curve from the positive sample (0.1 pg/mL α -syn oligomer containing Ab-H1, Ab-H2, MB1, MB2) displayed an apparent significant electrochemical signal (curve a), commencing with the splitting of MB3 and synthesis of many Fc localized around the GE surface. The combination's electrochemical intensity (curve b) was comparable to a blank (curve c), demonstrating the lack of the target human α -syn oligomer and demonstrating the absence of a DNAzyme-driven molecular machine. Additional control trials were also conducted for the proof-of-concept analysis. When we cultivated 0.1 pg/mL of α -syn oligomer in the reaction solution without the presence of Ab-H1 and Ab-H2, no signal was visible (curve d). The process of walker self-assembly required the Ab-H1-syn oligomer-Ab-H2-molecule, and this work demonstrated that MB1 and MB2 exhibit

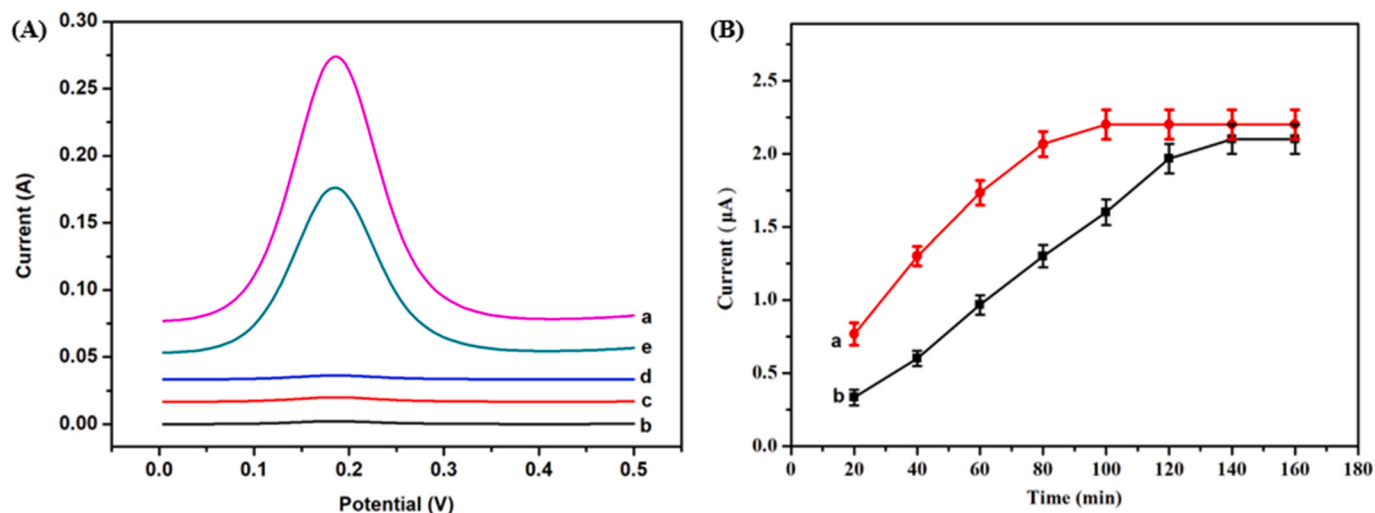


Fig. 2. (A) The DPV response of the sensor obtained by analyzing α -syn oligomers (a); curves b-e were for the control experiments carried out (b) without α -syn oligomers; (c) α -syn oligomers without MB0; (d) α -syn oligomers without MB1; (e) α -syn oligomers without MB2; (B) Electrochemical responses of the bipedal DNA walker, and bipedal walker (α -syn oligomers concentration: 0.1 pg/mL).

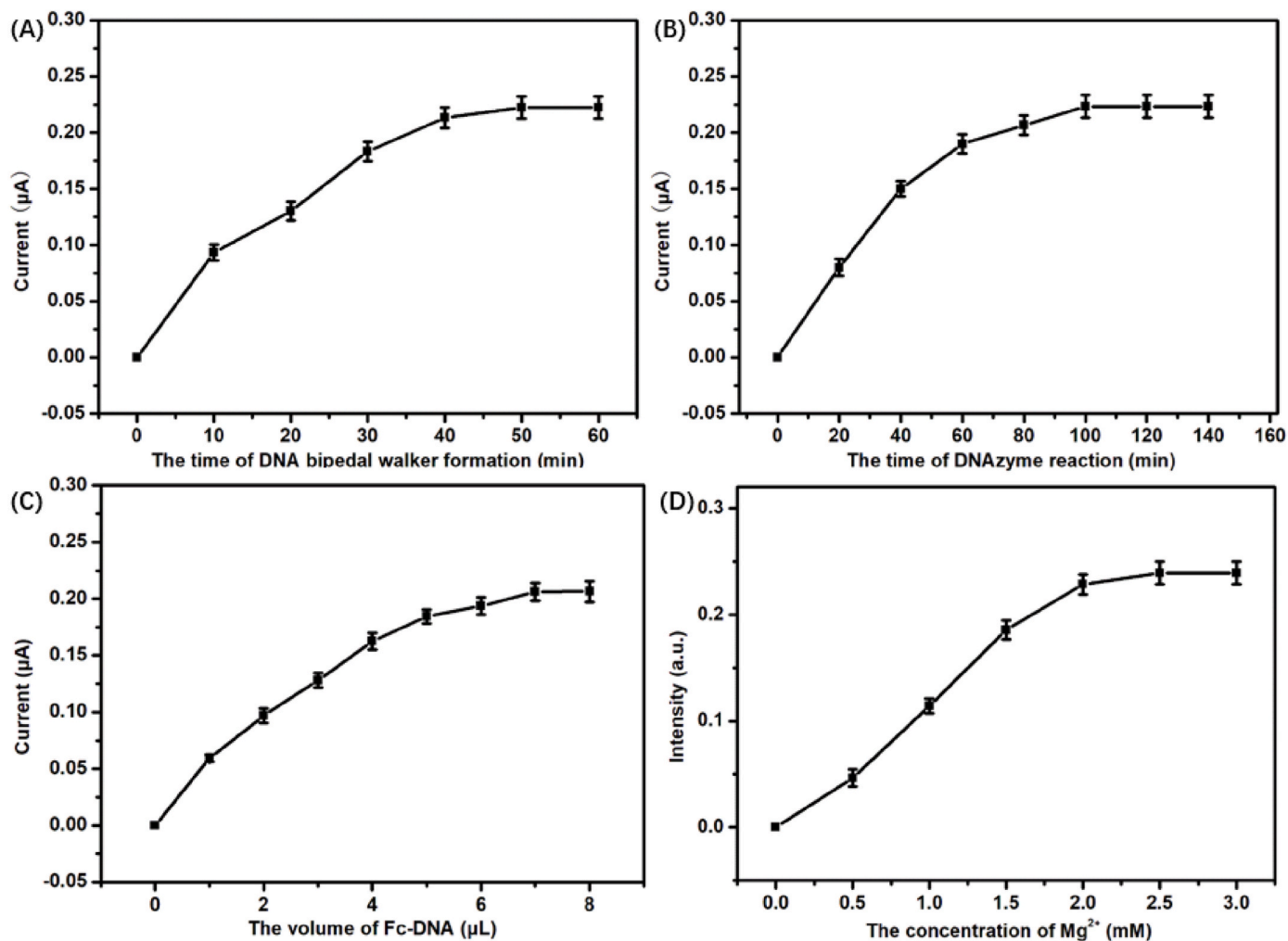


Fig. 3. Effect of (A) the time of DNA bipedal walker formation, (B) the time of DNAzyme reaction, (C) the amount of Fc-DNA, and (D) the amount of Mg^{2+} incubation on the performance of the electrochemical sensor.

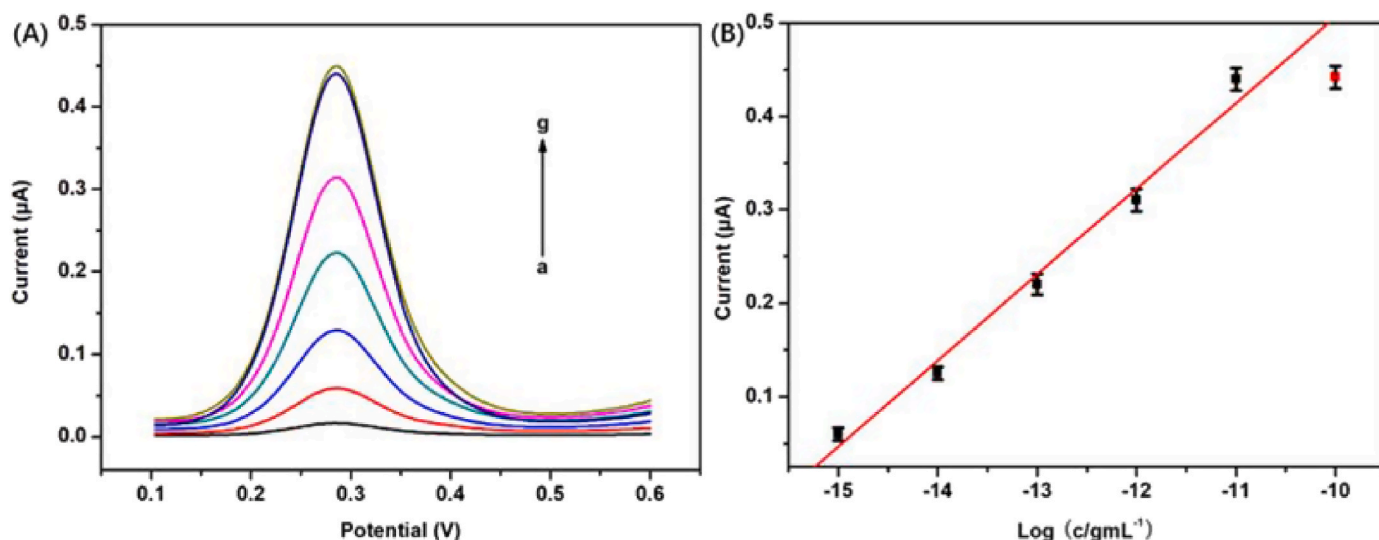


Fig. 4. (A) DPV responses and (B) standard calibration curve of the sensor after incubation with target α -syn oligomers ranging from 10^{-16} to 10^{-10} g/mL (curves (a)–(f)).

Table 1

Comparison of the proposed electrochemical sensor with previous works.

Detection methods	Linear range	Detection limit	Reference
Electrochemical	0.0526 pM–105.06 pM	0.0457 pM	48
Electrochemical	60 pM–150000 pM	10 pM	49
Electrochemical	60 pM - 150 nM	10 pM	50
Organic Field-Effect Transistor	0.25 pM–25 nM	0.25 pM	51
Surface plasmon resonance	70 nM–0.7 μM	70 nM	52
Electrochemical	10^{-4} –8 ng/mL	3.5×10^{-5} ng/mL	53
Electrochemical	4–2000 pg/mL	0.135 pg/mL	54
Electrochemical	1 fg/mL ~0.1 ng/mL	0.57 fg/mL	This work

exceptional robustness in the assay. A significantly higher electrochemical signal (curve e) was discovered when 0.1 pg/mL of α -syn oligomer was incubated in the reaction without the addition of MB2. This showed that the bipedal DNA walker was moving faster than the

single-legged DNA walker. The results show that the two-legged DNA walker is more effective than the single-legged one, but less effective than the bipedal one. Inferring that the efficiency of walking increased as the number of legs increased. Fig. 2B displays the findings of the comparison. In 100 min, the bipedal DNA walker achieved equilibrium. Compared with the single-leg walker, the multi-leg DNA walker can shorten the running time and amplify the output signal because of its higher space efficiency and better dynamic parameters. Therefore, the biped sensor has a high sensitivity and can be used to quantify α -syn oligomers.

3.4. The optimization process of experimental parameters

There are four factors that affected detection were the bipedal walker's evolution (the DNAzyme reaction, the amount of Fc-DNA present, and the Fc-DNA's incubation time). In order to obtain the best sensing performance, the effect of reaction kinetics under different experimental parameters was investigated. The current increased with the hybridization reaction time and then leveled off at 50 min (Fig. 3A).

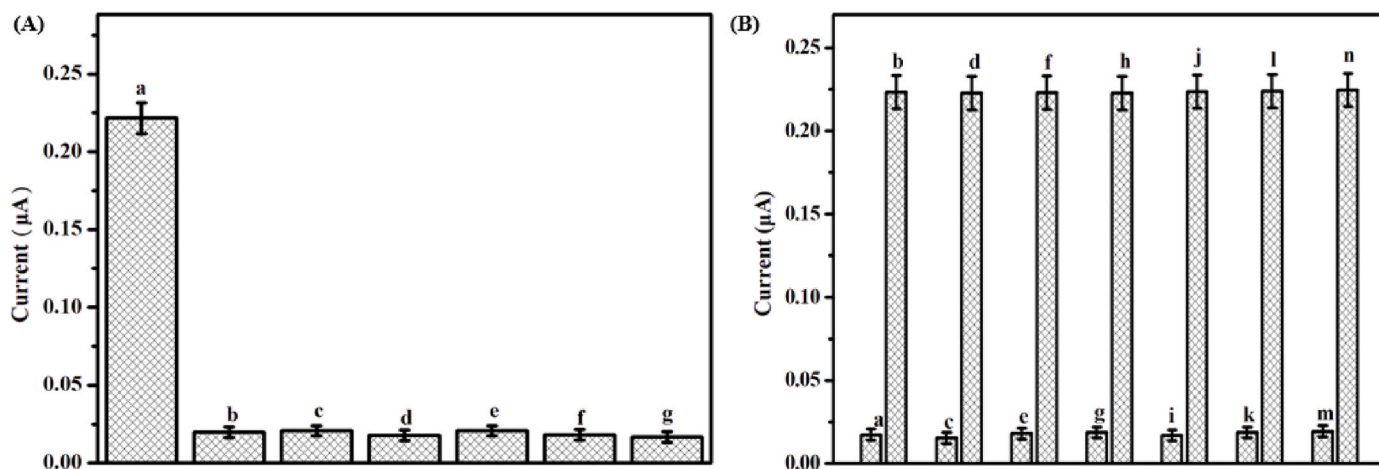


Fig. 5. (A) Histogram of the selectivity of the sensor evaluated through following samples: (a) 0.1 pg/mL α -syn oligomer; (b) blank; (c) 1 pg/mL A β O; (d) 1 pg/mL A β F; (e) 1 pg/mL A β M; (f) 1 pg/mL IgG and (g) 1 pg/mL BSA. (B) Histogram of interfering effects of different sample matrixes (a) blank; (b) 0.1 pg/mL α -syn oligomer; (c) 1 pg/mL potassium; (d) 1 pg/mL potassium + 0.1 pg/mL α -syn oligomer; (e) 1 pg/mL chloride; (f) 1 pg/mL chloride + 0.1 pg/mL α -syn oligomer; (g) 1 pg/mL glucose; (h) 1 pg/mL glucose + 0.1 pg/mL α -syn oligomer; (i) 1 pg/mL uric acid; (j) 1 pg/mL uric acid + 0.1 pg/mL α -syn oligomer; (k) 1 pg/mL dopamine and (l) 1 pg/mL dopamine + 0.1 pg/mL α -syn oligomer; (m) 1 pg/mL calcium ions; (n) 1 pg/mL calcium ions + 0.1 pg/mL α -syn oligomer.

Table 2

Detection of α -Syn oligomers in human serum sample using the developed sensor.

Added amounts	Found amounts	Recovery (%)	RSD
1 fg/mL	1.042 fg/mL	104.2	3.54
10 fg/mL	10.52 fg/mL	105.2	3.21
100 fg/mL	103.8 fg/mL	103.8	2.65
1 pg/mL	0.973 pg/mL	97.3	4.21
10 pg/mL	10.29 pg/mL	102.9	3.18

It was shown that the optimal assembly time of DNA bipedal walkers was 50 min. As the response time lengthened in Fig. 3B, the current shot up quickly before leveling out at balance. Therefore, the proper time for the DNAzyme reaction was 100 min. To investigate the optimal dose of Fc-DNA, we used different concentrations of Fc-DNA for incubation GE. The current gradually increased with the aid of Fc-DNA, and 7 μ L was found to be the suitable dose of Fc-DNA (Fig. 3C). In Fig. 3D, according to the same principle, the appropriate Mg^{2+} concentration is 2.5 mM.

3.5. Performance of the sensor

Under optimal conditions, the sensors were incubated with varying concentrations of α -syn oligomer, and their electrochemical responses were recorded. It was shown in Fig. 4A that electrochemical signal rose as α -syn oligomer concentrations rose. The typical calibration curve was displayed in Fig. 4B. From 1 fg/mL to 0.1 ng/mL, the dosage response curve showed a strong linear relationship. The linear equation was $I = 1.39 + 0.09 \log c$ (where c stood for α -syn oligomer concentrations and I for the current) and had a correlation coefficient of 0.9832. Nonspecific emission could be decreased in comparison to other sensor approaches (Table 1), and this detection method did not necessitate the development of a nanocomposite probe. The successful construction and good performance of sensors may be attributed to two fold signal amplification, which rendered it easier to foster Fc proliferation on the GE surface.

3.6. Specificity of the sensor

It is crucial to examine how the probes respond to a number of similar interfering or coexisting substances in order to evaluate the developed sensor's selectivity for detecting α -syn oligomers in a complicated biological environment. To conduct the experiment utilizing the biosensor under the same conditions, we selected amyloid- β oligomers (A β O), amyloid- β fibers (A β F), amyloid- β monomer (A β M), immunoglobulin G (IgG), L-cysteine, and bovine serum albumin (BSA). In Fig. 5A, the addition of α -syn oligomers led to a strong current response, but other compounds, even at high concentrations, virtually had no effect on the current response. According to the results above, the α -syn oligomer had a better affinity and selectivity for conjugating to its antibody than other non-specific molecules.

The response of our created sensor method was examined in the presence of a number of sample matrix components, including K^+ , Cl^- , Glu, UA, and DA. These components were all probable interfering components in the normal human blood sample. Instead of using serum blood samples directly, we used individual interfering component to examine its impact on the detection of α -syn oligomers. The low concentration of target α -syn oligomers and the high concentration of interfering components were evaluated in the comparison investigation in line with the current shift in the absence and presence of interfering reagents. The current intensities determined from K^+ , Cl^- , Glu, UA, and DA alone were almost equal to the background signal, as shown in Fig. 5B. In addition, in contrast to the pure target analytes, the electrochemical signals were not significantly increased when interfering reagents were combined with α -syn oligomers. Based on these experimental findings, it was possible to draw the conclusion that the serum sample matrix components did not significantly affect the detection

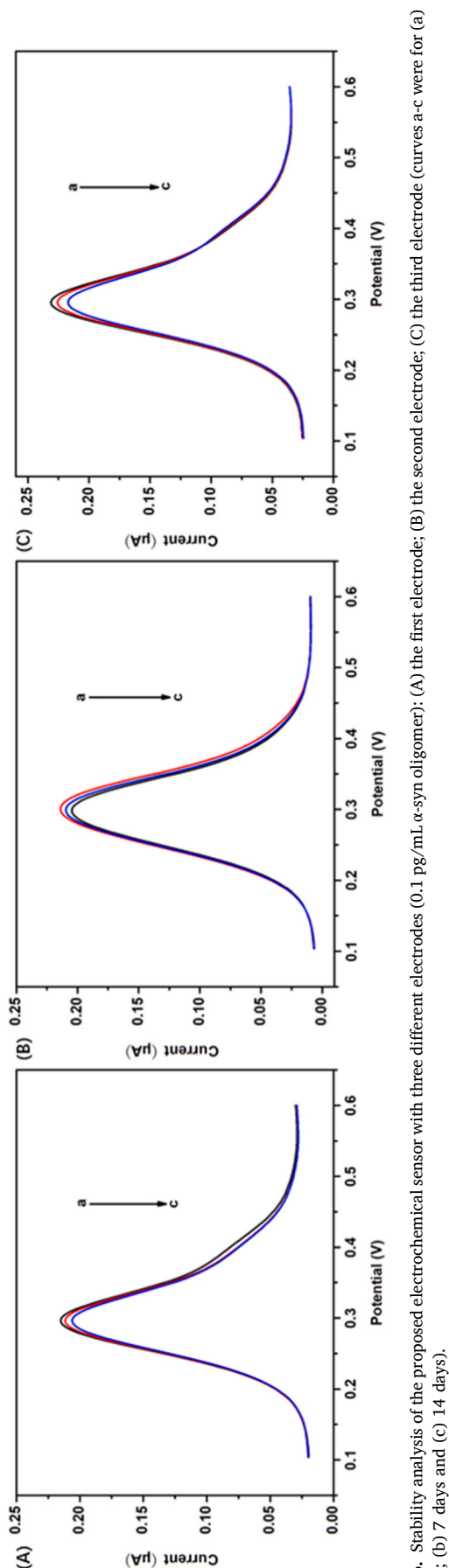


Fig. 6. Stability analysis of the proposed electrochemical sensor with three different electrodes (A) the first electrode; (B) the second electrode; (C) the third electrode (curves a-c were for (a) 0 day; (b) 7 days and (c) 14 days).

process's ability to quantify α -syn oligomers. Excellent selectivity and anti-interference characteristics of the electrochemical sensor for α -syn oligomer detection point to its enormous potential for practical use in challenging biological contexts.

3.7. Application in detection of clinical serum samples

The assay was performed on serum samples with known α -syn oligomer concentrations to evaluate the practical clinical potential. Relative standard deviations (RSDs) ranged between 2.65 % and 4.21 %, and it was observed that recoveries fluctuated between 97.3 and 105.2 % (Table 2). These findings suggested that the electrochemical sensor may identify α -syn oligomer in actual samples.

3.8. Reproducibility and stability of the sensor

If the sensor might be employed in clinical practice, it would depend on its reproducibility and stability over time. Two weeks had been spent testing the stability of the suggested procedure. Following every measurement, the sensor was kept in a buffer solution (Tris-HCl) at 4 °C. For a period of around 2 weeks, the value of I_{Fc} was monitored intermittently by measuring it every 2 days. The sensor remained able to sustain no less than 96 % of the initial response, as shown in Fig. 6, demonstrating that the manufactured sensors had developed a level of stability appropriate for α -syn oligomer detection. According to aforementioned findings, this sensor demonstrated high repeatability.

4. Conclusion

In summary, we have created an electrochemical biosensor for the detection of α -syn oligomers based on proximity hybridization triggering DNAzyme driven. The proposed method displayed great sensitivity, and its detection limit was 0.57 fg/mL due to the effective dual signal amplification methodology used by bipedal DNA walker and DNAzyme. Furthermore, the serum α -syn oligomer sensor could be utilized in clinical serum samples with potential for clinical translation. This strategy can also be used to construct diverse bipedal DNA walkers by adjusting the appropriate DNA ligand sequence, demonstrating its important application prospects for the identification of a range of targets.

CRedit authorship contribution statement

Qisheng Luo: Methodology, Investigation. **Zhili Qiu:** Methodology, Investigation. **Hongqu Liang:** Data curation. **Fa Huang:** Methodology. **Chen Wei:** Formal analysis. **Jiuying Cui:** Formal analysis. **Zichun Song:** Formal analysis, Data curation. **Qianli Tang:** Investigation. **Xianjiu Liao:** Formal analysis, Data curation. **Zhao Liu:** Methodology, Investigation. **Jiangbo Wang:** Resources, Software. **Fenglei Gao:** Visualization, Validation, Supervision.

Declaration of competing interest

The authors declare that they have no known competing financial interests or personal relationships that could have appeared to influence the work reported in this paper.

Data availability

Data will be made available on request.

Acknowledgements

We gratefully acknowledge the financial support of Xuzhou Science and Technology Project (KC22067), the National Natural Science Foundation of China (21964018 and 82360259), the Guangxi key

laboratory of basic and translational research of bone and joint degenerative disease (21-220-06-202205), the State Key Laboratory of Analytical Chemistry for Life Science (SKLACLS2314).

Appendix A. Supplementary data

Supplementary data to this article can be found online at <https://doi.org/10.1016/j.talanta.2024.125720>.

References

- [1] A. Samii, J.G. Nutt, B.R. Ransom, Parkinson's disease, *Lancet* 363 (2004) 1783–1793.
- [2] Q. Chen, Y.X. Xue, Y.L. Huang, W.Y. Guo, M.M. Wan, J. Shen, Mg-based micromotors for electrochemical detection of Parkinson's disease blood biomarkers, *Sensor. Actuator. B Chem.* 402 (2024) 135035.
- [3] G. Gimenez-Aparisi, E. Guíjarro-Estelles, A. Chornet-Lurbe, S. Ballesta-Martínez, M. Pardo-Hernández, Y. Ye-Lin, Early detection of Parkinson's disease: systematic analysis of the influence of the eyes on quantitative biomarkers in resting state electroencephalography, *Heliyon* 9 (2023) e20625.
- [4] H.V.S. Ganesh, A.M. Chow, K. Kerman, Recent advances in biosensors for neurodegenerative disease detection, *TRAC-Trend. Anal. Chem.* 79 (2016) 363.
- [5] M.R. Sierks, G. Chatterjee, C. McGraw, S. Kasturirangan, P. Schulz, S. Prasad, CSF levels of oligomeric alpha-synuclein and beta-amyloid as biomarkers for neurodegenerative disease, *Integr. Biol.* 3 (2011) 1188.
- [6] S.M. Williams, P. Schulz, M.R. Sierks, Oligomeric α -synuclein and β -amyloid variants as potential biomarkers for Parkinson's and Alzheimer's diseases, *Eur. J. Neurosci.* 43 (2016) 3.
- [7] E.B.M. Ladinska, Parkinson's disease: diagnostic relevance of elevated levels of soluble α -synuclein oligomers in cerebrospinal fluid, *Future Neurol.* 6 (2011) 159.
- [8] O. Hansson, S. Hall, A. Öhrfelt, H. Zetterberg, K. Blennow, L. Minthon, K. Nägga, E. Londos, S. Varghese, N.K. Majbour, A. Al-Hayani, O.M. El-Agnaf, Levels of cerebrospinal fluid-synuclein oligomers are increased in Parkinson's disease with dementia and dementia with Lewy bodies compared to Alzheimer's disease, *Alzheimer's Res. Ther.* 6 (2014) 25.
- [9] M.J. Park, S.-M. Cheon, H.-R. Bae, S.-H. Kim, K.J. W, Elevated levels of α -synuclein oligomer in the cerebrospinal fluid of drug-naïve patients with Parkinson's disease, *J. Clin. Neurol.* 7 (2011) 215.
- [10] X. Wang, S. Yu, F. Li, T. Fengm, Detection of α -synuclein oligomers in red blood cells as a potential biomarker of Parkinson's disease, *Neurosci. Lett.* 599 (2015) 115.
- [11] A. Idili, A. Amodio, M. Vidonis, J. Feinberg-Somerson, M. Castronovo, F. Ricci, Folding-upon-binding and signal-on electrochemical DNA sensor with high affinity and specificity, *Anal. Chem.* 86 (2014) 9013–9019.
- [12] F.Q. Li, Z.G. Yu, H.C. Qu, G.L. Zhang, H. Yan, X. Liu, X.J. He, A highly sensitive and specific electrochemical sensing method for robust detection of *Escherichia coli* lac Z gene sequence, *Biosens. Bioelectron.* 68 (2015) 78–82.
- [13] C.H. Fan, K.W. Plaxco, A.J. Heeger, Electrochemical interrogation of conformational changes as a reagentless method for the sequence-specific detection of DNA, *Proc. Natl. Acad. Sci. USA* 100 (2003) 9134–9137.
- [14] Q. Wang, L. Yang, X. Yang, K. Wang, L. He, J. Zhu, T. Su, An electrochemical DNA biosensor based on the Y junction structure and restriction endonuclease-aided target recycling strategy, *Chem. Commun.* 48 (2012) 2982–2984.
- [15] J.C. Cunningham, N.J. Brenes, R.M. Crooks, Paper electrochemical device for detection of DNA and thrombin by target-induced conformational switching, *Anal. Chem.* 86 (2014) 6166–6170.
- [16] X.M. Miao, X.T. Guo, Z.Y. Xiao, L.S. Ling, Electrochemical molecular beacon biosensor for sequence-specific recognition of double-stranded DNA, *Biosens. Bioelectron.* 59 (2014) 54–57.
- [17] F. Ricci, R.Y. Lai, K.W. Plaxco, Linear, redox modified DNA probes as electrochemical DNA sensors, *Chem. Commun.* 43 (2007) 3768–3770.
- [18] A.A. Lubin, R.Y. Lai, B.R. Baker, A.J. Heeger, K.W. Plaxco, Sequence-specific electronic detection of oligonucleotides in blood, soil, and foodstuffs with the reagentless, reusable E-DNA sensor, *Anal. Chem.* 78 (2006) 5671–5677.
- [19] A. Anne, A. Bouchardon, J. Moiroux, 30-Ferrocene-labeled oligonucleotide chains end-tethered to gold electrode surfaces: novel model systems for exploring flexibility of short DNA using cyclic voltammetry, *J. Am. Chem. Soc.* 125 (2003) 1112–1113.
- [20] Z.L. Shen, S. Nakayama, S. Semancik, H.O. Sintim, Signal-on electrochemical Y or junction probe detection of nucleic acid, *Chem. Commun.* 48 (2012) 7580–7582.
- [21] Y. Wu, R.Y. Lai, Development of a signal-on electrochemical DNA sensor with an oligo-thymine spacer for point mutation detection, *Chem. Commun.* 49 (2013) 3422–3424.
- [22] P. Zhang, T. Beck, W.H. Tan, Design of a molecular beacon DNA probe with two fluorophores, *Angew. Chem. Int. Ed.* 40 (2001) 402–405.
- [23] H.R. Zhang, J.J. Xu, H.Y. Chen, Electrochemiluminescence ratiometry: a new approach to DNA biosensing, *Anal. Chem.* 85 (2013) 5321–5325.
- [24] Y. Cheng, Y. Huang, J.P. Lei, L. Zhang, H.X. Ju, Design and biosensing of Mg^{2+} -dependent DNAzyme-triggered ratiometric electrochemiluminescence, *Anal. Chem.* 86 (2014) 5158–5163.
- [25] Y. Du, B.J. Lim, B.L. Li, Y.S. Jiang, J.L. Sessler, A.D. Ellington, Reagentless, ratiometric electrochemical DNA sensors with improved robustness and reproducibility, *Anal. Chem.* 86 (2014) 8010–8016.

- [26] P. Zhang, J. Jiang, R. Yuan, Y. Zhuo, Y.Q. Chai, Highly ordered and field-free 3D DNA nanostructure: the next generation of DNA nanomachine for rapid single-step sensing, *J. Am. Chem. Soc.* 140 (2018) 9361–9364.
- [27] W.T. Yang, Y. Shen, D.Y. Zhang, C. Li, R. Yuan, W.J. Xu, Programmed dual-functional DNA tweezer for simultaneous and recognizable fluorescence detection of microRNA and protein, *Anal. Chem.* 91 (2019) 7782–7789.
- [28] T.T. Wu, Y. Cao, Y.M. Yang, X.Y. Zhang, S.T. Wang, L.P. Xu, X.J. Zhang, A three-dimensional DNA walking machine for the ultrasensitive dual-modal detection of miRNA using a fluorometer and personal glucose meter, *Nanoscale* 11 (2019) 11279–11284.
- [29] C.J. Sui, Y.L. Zhou, M.Y. Wang, H.S. Yin, P. Wang, S.Y. Ai, Aptamer-based photoelectrochemical biosensor for antibiotic detection using ferrocene modified DNA as both aptamer and electron donor, *Sensor. Actuator. B Chem.* 266 (2018) 514–521.
- [30] Y.Y. Li, G.A. Wang, S.D. Mason, X.L. Yang, Z.C. Yu, Y.Y. Tang, F. Li, Simulation-guided engineering of an enzyme-powered three dimensional DNA nanomachine for discriminating single nucleotide variants, *Chem. Sci.* 9 (2018) 6434–6439.
- [31] P.Q. Ma, C.P. Liang, H.H. Zhang, B.C. Yin, B.C. Ye, A highly integrated DNA nanomachine operating in living cells powered by an endogenous stimulus, *Chem. Sci.* 9 (2018) 3299–3304.
- [32] C. Liu, Y. Hu, Q. Pan, J. Yi, J. Zhang, M. He, M. He, T. Chen, X. Chu, A microRNA-triggered self-powered DNAzyme walker operating in living cells, *Biosens. Bioelectron.* 136 (2019) 31–37.
- [33] Y. Chang, Z. Wu, Q. Sun, Y. Zhuo, Y. Chai, R. Yuan, Simply constructed and highly efficient classified cargo-discharge DNA robot: a DNA walking nanomachine platform for ultrasensitive multiplexed sensing, *Anal. Chem.* 91 (2019) 8123–8128.
- [34] J.Y. Zhu, B.S. He, Y. Liu, Y.L. Wang, J.S. Wang, Y. Liang, H.L. Jin, M. Wei, W. J. Ren, Z.G. Suo, Y.W. Xu, A novel magneto-mediated electrochemical biosensor integrated DNAzyme motor and hollow nanobox-like Pt@Ni-Co electrocatalyst as dual signal amplifiers for vanilla detection, *Biosens. Bioelectron.* 241 (2023) 115690.
- [35] A. Chen, Y. Zhuo, Y. Chai, R. Yuan, Bipedal DNA walker mediated enzyme-free exponential isothermal signal amplification for rapid detection of microRNA, *Chem. Commun.* 55 (2019) 13932–13935.
- [36] Z. Xu, Y. Chang, Y. Chai, H. Wang, R. Yuan, Ultrasensitive electrochemiluminescence biosensor for speedy detection of microRNA based on a DNA rolling machine and target recycling, *Anal. Chem.* 91 (2019) 4883–4888.
- [37] H. Zhang, X. Xu, W. Jiang, An interparticle relatively motional DNA walker and its sensing application, *Chem. Sci.* 11 (2020) 7415–7423.
- [38] P. Miao, Y. Tang, Gold nanoparticles-based multipedal DNA walker for ratiometric detection of circulating tumor cell, *Anal. Chem.* 91 (2019) 15187–15192.
- [39] D. Li, Y. Xu, L. Fan, B. Shen, X. Ding, R. Yuan, X. Li, W. Chen, Target-driven rolling walker based electrochemical biosensor for ultrasensitive detection of circulating tumor DNA using doxorubicin@tetrahedron-Au tags, *Biosens. Bioelectron.* 148 (2020) 111826.
- [40] H.Q. Zhang, F. Li, B. Dever, C. Wang, X.F. Li, X.C. Le, Assembling DNA through affinity binding to achieve ultrasensitive protein detection, *Angew. Chem. Int. Ed.* 52 (2013) 10698–10705.
- [41] H.Q. Zhang, F. Li, B. Dever, X.F. Li, X.C. Le, DNA-mediated homogeneous binding assays for nucleic acids and proteins, *Chem. Rev.* 113 (2013) 2812–2841.
- [42] D. Li, Y. Li, F. Luo, B. Qiu, Z.Y. Lin, Ultrasensitive homogeneous electrochemiluminescence biosensor for a transcription factor based on target-modulated proximity hybridization and exonuclease III-powered recycling amplification, *Anal. Chem.* 92 (2020) 12686–12692.
- [43] J.L. Li, M.Q. Yang, D. Cao, L. Zhang, C. Zong, P. Li, Ultrasensitive homogeneous detection of PCSK9 and efficacy monitoring of the PCSK9 inhibitor based on proximity hybridization-dependent chemiluminescence imaging immunoassay, *Anal. Chem.* 95 (2023) 5428–5435.
- [44] Y.X. Wei, J. Zhang, X.L. Yang, Z.M. Wang, J.X. Wang, H.L. Qi, Q. Gao, C.X. Zhang, Washing-free electrogenerated chemiluminescence magnetic microbiosensors based on target assistant proximity hybridization for multiple protein biomarkers, *Anal. Chim. Acta* 1253 (2023) 340926.
- [45] X.F. Wang, H.F. Gao, H.L. Qi, Q. Gao, C.X. Zhang, Proximity hybridization-regulated immunoassay for cell surface protein and protein-overexpressing cancer cells via electrochemiluminescence, *Anal. Chem.* 90 (2018) 3013–3018.
- [46] X.J. Liao, C.Y. Zhang, J.O. Machuki, X.Q. Wen, Q.L. Tang, H.L. Shi, F.L. Gao, Proximity hybridization-triggered DNA assembly for label-free surface-enhanced Raman spectroscopic bioanalysis, *Anal. Chim. Acta* 1139 (2020) 42–49.
- [47] Y. Qian, T.T. Fan, P. Wang, X. Zhang, J.J. Luo, F.Y. Zhou, Y. Yao, X.J. Liao, Y.H. Li, F.L. Gao, A novel label-free homogeneous electrochemical immunosensor based on proximity hybridization-triggered isothermal exponential amplification induced G-quadruplex formation, *Sensor. Actuator. B Chem.* 248 (2017) 187–194.
- [48] C.P. Guo, M.Y. Hu, Z.Z. Li, F.H. Duan, L.H. He, Z.H. Zhang, F. Marchetti, M. Du, Structural hybridization of bimetallic zeolitic imidazolate framework (ZIF) nanosheets and carbon nanofibers for efficiently sensing α -synuclein oligomers, *Sensor. Actuator. B Chem.* 309 (2020) 127821.
- [49] S.M. Taghdisi, N.M. Danesh, M.A. Nameghi, M. Ramezani, M. Alibolandi, M. Hassanzadeh-Khayat, A.S. Emrani, K. Abnous, A novel electrochemical aptasensor based on nontarget-induced high accumulation of methylene blue on the surface of electrode for sensing of α -synuclein oligomer, *Biosens. Bioelectron.* 123 (2019) 14–18.
- [50] S.M. Taghdisi, N.M. Danesh, M.A. Nameghi, M. Ramezani, M. Alibolandi, M. Hassanzadeh-Khayat, A.S. Emrani, K. Abnous, A novel electrochemical aptasensor based on nontarget-induced high accumulation of methylene blue on the surface of electrode for sensing of α -synuclein oligomer, *Biosens. Bioelectron.* 123 (2019) 14–18.
- [51] S. Ricci, S. Casalini, V. Parkula, M. Selvaraj, G.D. Saygin, P. Greco, F. Biscarini, M. Mas-Torrent, Label-free immunodetection of α -synuclein by using a microfluidics coplanar electrolyte-gated organic field-effect transistor, *Biosens. Bioelectron.* 167 (2020) 112433.
- [52] A. Khatri, N. Punjabi, D. Ghosh, S.K. Maji, S. Mukherji, Detection and differentiation of α -Synuclein monomer and fibril by chitosan film coated nanogold array on optical sensor platform, *Sens. Actuators, B* 255 (2018) 692–700.
- [53] Y. Ma, Q. Hu, C. Liu, L. Wang, A nanospherical conjugated microporous polymer-graphene nanosheets modified molecularly imprinted electrochemical sensor for high sensitivity detection of α -Synuclein, *J. Electroanal. Chem.* 862 (2020) 113994.
- [54] M.N. Sonuç Karaboga, M.K. Sezginç, Cerebrospinal fluid levels of alpha-synuclein measured using a poly-glutamic acid-modified gold nanoparticle-doped disposable neuro-biosensor system, *Analyst* 144 (2019) 611–621.